

Thermodynamic modeling and life cycle assessment of limestone calcined clay cements

Pham Hoai My^{1,2}, Nguyen Thi Bich Hong^{1,2}, Ho Viet Thang^{1,2*}

¹ Faculty of Chemical Engineering, The University of Danang, University of Science and Technology

² Strategic Materials & Advanced Research Team – DUT (SMART-DUT), The University of Danang, University of Science and Technology

KEYWORDS

LC3 Cement
Hydration
Calcined clay
Sustainability
Durability

ABSTRACT

To meet the net-zero CO₂ goal by 2050, low-carbon construction materials like limestone calcined clay cement (LC3), which replaces a large portion of clinker with calcined clay and limestone, are essential. This study used thermodynamic modeling and life cycle assessment to evaluate a range of LC3 formulations with clinker content from 65% to 35%. Results show aluminate-CaCO₃ interaction forms stable carboaluminate phases, leading to a denser microstructure. While lower clinker content leads to a decrease in pH and solid volume, the LC3-50 mixture achieved the optimal balance between hydration product stability and material efficiency. LCA confirms that reduced clinker content significantly lowers environmental impacts across all indicators, most notably achieving a 32.92% reduction in global warming potential and a 40.78% reduction in ozone depletion potential. These findings offer a scientific basis for optimizing LC3 mixtures and promoting its use as a sustainable building material.

1. Introduction

Due to the global transition toward net-zero CO₂ emissions by 2050,[1] the cement industry is confronted with significant pressure to mitigate its energy consumption and carbon footprint. The manufacturing of traditional ordinary Portland cement (OPC) necessitates the use of clinker fired at elevated temperatures, a procedure that is highly energy-intensive due to the reliance on fossil fuels, and simultaneously generates substantial quantities of CO₂ through the thermal decomposition of limestone. [2] Furthermore, cement production results in the emission of dust, nitrogen oxides (NO_x), and sulfur oxides (SO_x), contributing heavily to air pollution, resource depletion, and environmental degradation.[3] To align with the ultimate goal of net-zero emissions by 2050, the International Energy Agency (IEA) has outlined a transition pathway requiring cement manufacturers to reduce their carbon intensity by approximately 0.3 % annually up to the 2030 milestone.[4] Consequently, cement plants failing to adopt low-carbon manufacturing processes and energy-efficiency measures may face sanctions for non-compliance with environmental regulations and miss cost-saving opportunities related to process innovation.

To address these environmental burdens, the development of low-clinker binder systems, notably limestone calcined clay cement (LC3),[5], [6] has emerged as a crucial research direction. LC3 aims to mitigate environmental impacts while ensuring the stringent technical requirements necessary for modern construction.[7], [8], [9] Parallel to the development of these new eco-friendly materials, the methodology for studying and evaluating cementitious properties is undergoing a

major paradigm shift from traditional experimental testing to advanced simulation and modeling tools. Although laboratory experiments provide direct and reliable data, they are often associated with high material consumption, high costs, and extended testing durations. Moreover, the real-time observation of hydration reactions at the micro-level remains technically limited.

In contrast, thermodynamic simulation methods allow for the robust prediction of phase formation, phase transformation, and the evolution of porosity and microstructure over time, offering lower costs and significantly faster processing. Simulation is not intended to completely replace experiments but serves as a powerful complementary tool, helping to reduce the required number of empirical trials, optimize mix proportions prior to physical testing, and deepen the fundamental understanding of reaction mechanisms in complex multi-component systems like LC3. Among current simulation tools, the CemGEMS (Cement Gibbs Energy Minimization Software) [10] is widely utilized to model thermodynamic equilibrium and predict the hydration pathways of cementitious systems. This platform operates on the principle of minimizing the Gibbs free energy to determine the stable equilibrium state of multi-phase systems.

Although thermodynamic models have been successfully applied in numerous studies concerning OPC, their application to the LC3 system remains limited due to the thermodynamic complexity of reactions involving reactive aluminate phases and the subsequent formation of carboaluminate compounds. Furthermore, most current research focuses primarily on microstructural evolution and reaction mechanisms, while comprehensive assessments of the environmental impacts are often performed separately using life cycle assessment

*Corresponding author: hvthang@dut.udn.vn

Received 09/04/2026, revised 17/05/2026, accepted 18/05/2026

Link DOI: <https://doi.org/10.54772/jomc.v16i01.1320>

(LCA).[11] Given these isolated approaches, combining thermodynamic simulation using CemGEMS application with LCA is essential for a holistic evaluation of both the technical performance and the sustainability of the LC3 system. Therefore, this study aims to simulate the hydration process of LC3 to elucidate the mechanisms of product phase formation, while simultaneously quantifying its environmental impacts relative to OPC. These integrated findings will provide a solid scientific basis for optimizing LC3 mixture proportions and guiding the future deployment of sustainable green cement materials.

2. Materials and Methods

2.1. Materials

The chemical compositions of clinker, limestone, and calcined clay were adopted from the standardized recipes in the CemGEMS application,[10] which are consistent with the Cemdata18 thermodynamic database.[12] The composition of these materials is reported in Table 1.

To evaluate the effect of various LC3, a range of LC3 with different clinker content from 65 % to 35 % are applied in this study (Table 2).

Table 1. Chemical composition of clinker, calcined clay and limestone (wt.%).

Composition	Clinker	Calcined clay	Limestone
CaO	67.92	0.10	42.30
SiO ₂	21.91	53.55	12.40
Al ₂ O ₃	4.80	44.08	2.70
Fe ₂ O ₃	2.77	0.31	2.00
MgO	0.98	-	1.80
Na ₂ O	0.09	0.31	0.50
K ₂ O	0.76	0.10	0.60
SO ₃	0.77	-	-
LOI	-	1.54	37.70

Table 2. Mix proportions of OPC and LC3 systems (wt.%).

System	Clinker	Calcined clay	Limestone	Gypsum
OPC	95	-	-	5
LC3-65	65	15	15	5
LC3-60	60	20	15	5
LC3-55	55	25	15	5
LC3-50	50	30	15	5
LC3-45	45	35	15	5
LC3-40	40	40	15	5
LC3-35	35	45	15	5

2.2. Thermodynamic Modeling

Thermodynamic equilibrium calculations were performed using the CemGEMS web application, utilizing the GEMS3K numerical kernel [13] and the Cemdata18 database.[12] The simulations were conducted under isothermal conditions at 27 °C and a pressure of 1 atm, with a constant water-to-binder (w/b) ratio of 0.40. The hydration process was simulated for ordinary Portland cement (OPC) and various LC3 formulations. To accurately represent the complex cementitious phases, appropriate solid solution models provided by the Cemdata18 database [12] were applied. This notably includes the C-N-K-S-H-ss model for the calcium silicate hydrate gel (referred to as C-(A)-S-H hereafter due to aluminum incorporation), as well as solid solutions for AFm, AFt, and hydrotalcite phases. Alongside these solid solutions, standard pure stoichiometric phases such as portlandite (CH), ettringite, and relevant unreacted minerals were computed to determine the total thermodynamically stable phase assemblage. Finally, the temporal evolution of the phase assemblages was modeled by defining the degree of hydration of the individual clinker phases and supplementary cementitious materials using the built-in empirical kinetic models of modified Parrot-Killoh equations provided by the CemGEMS platform.

2.3. Life Cycle Assessment

The environmental performance was evaluated through Life Cycle Assessment in accordance with ISO 14040/14044 standards, utilizing OpenLCA software.[11] A functional unit of 1 tonne of blended cement was selected to ensure comparability between the OPC and the various LC3 formulations. A 'cradle-to-gate' system boundary was defined, encompassing raw material extraction, clinker and clay calcination, grinding, and final blending. The life cycle inventory (LCI) data were primarily sourced from the Ecoinvent database [14] for LC3-specific processes such as clay calcination at lower temperatures. Specifically, for the clay calcination stage conducted within a thermal threshold of 600–800 °C, the inventory assumes a representative global industrial thermal energy mix consisting of 55 % coal, 35 % natural gas, and 10 % heavy fuel oil by energy share. The environmental impacts were calculated using the CML 2001 baseline life cycle impact assessment (LCIA) method.[15] The evaluation focused on six key environmental indicators, including Global Warming Potential (GWP) in kg CO₂ eq, Ozone Depletion Potential (ODP) in kg CFC-11 eq, Photochemical Ozone Creation Potential (POCP) in kg NMVOC eq, Acidification Potential (AP) in mol H⁺ eq, Eutrophication Potential (EP) in mol N eq, and Abiotic Depletion Potential for fossil resources (ADPF) in MJ.

3. Results and Discussion

3.1. Thermodynamic modeling of microstructural evolution

3.1.1. Temporal evolution of phase assemblages

Figures 1 through 8 illustrate the thermodynamic predictions of the solid phase assemblages for OPC and the various LC3 mixtures (from LC3-65 to LC3-35) over a hydration period of up to 1000 days. As a reference, the hydration of OPC (Figure 1) exhibits a conventional phase evolution. The unreacted clinker minerals (predominantly C_3S and C_2S) dissolve steadily, leading to the continuous precipitation of calcium silicate hydrate (C-S-H), the primary strength contributing phase, and a rapid, sustained accumulation of portlandite (CH). Furthermore, ettringite (AFt) forms early but partially converts to monosulfate (AFm) upon the depletion of available sulfate.

In contrast, the LC3 mixtures demonstrate a distinctly different hydration trajectory, driven by the synergistic pozzolanic reaction of calcined clay and the active participation of limestone. Due to the dilution effect from the reduced clinker content, the initial volume of C-S-H in LC3 is noticeably lower than in OPC. However, as hydration progresses, the reactive alumina and silica from calcined clay vigorously consume the portlandite generated by clinker hydration. This intense pozzolanic activity not only prevents the excessive accumulation of CH, a hallmark of LC3 mixtures that significantly enhances chemical durability but also promotes the formation of a highly cross-linked, aluminum-substituted C-(A)-S-H gel.

The most profound microstructural divergence in the LC3 mixtures is the stabilization of carboaluminate phases. The abundant supply of alumina from metakaolin reacts synergistically with calcium carbonate from the limestone. Consequently, while AFt forms early, the subsequent AFm phases follow a different thermodynamic pathway compared to OPC. Instead of forming monosulfate, the system strongly favors the precipitation of hemicarboaluminate (Hc), which progressively transforms into the thermodynamically more stable monocarboaluminate (Mc) phase. The sustained growth of Mc, particularly prominent in the mid-range LC3 mixtures (LC3-55, LC3-50, and LC3-45), plays a pivotal role in refining the pore structure and densifying the solid matrix.

Analyzing the effect of progressive clinker reduction reveals a clear thermodynamic trade-off. LC3 mixtures with severely reduced clinker (LC3-40, LC3-35) exhibit inadequate C-(A)-S-H formation and almost depletion of portlandite, which could compromise the long-term alkalinity and mechanical reserves of the cementitious matrix. Conversely, intermediate mixtures, specifically LC3-50, achieve a thermodynamic optimum. At this replacement level, the system maintains sufficient C-(A)-S-H generation for structural integrity, effectively consumes the vulnerable portlandite, and maximizes the volume of the space-filling monocarboaluminate phase. Therefore, the thermodynamic modeling validates that the LC3-50 blend provides the optimal synergy between hydration stability, material efficiency, and microstructural densification.

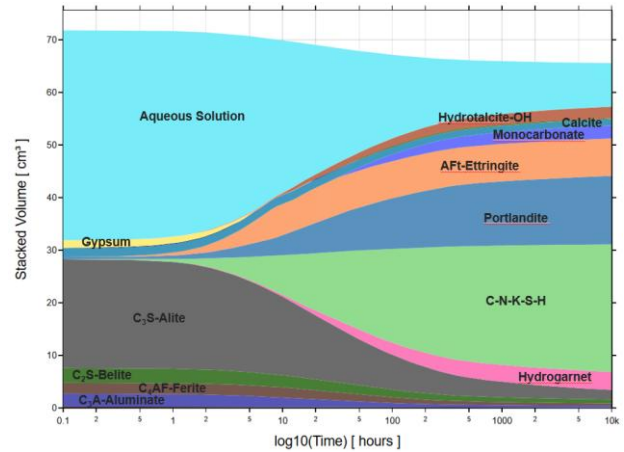


Figure 1. Thermodynamic simulation of solid phase evolution during the hydration of OPC.

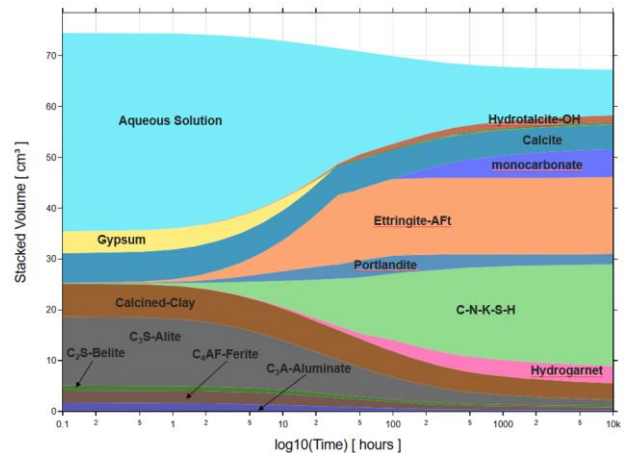


Figure 2. Thermodynamic simulation of solid phase evolution during the hydration of LC3-65.

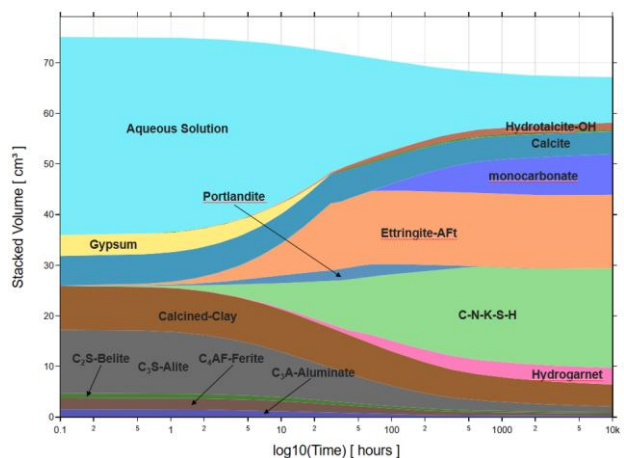


Figure 3. Thermodynamic simulation of solid phase evolution during the hydration of LC3-60.

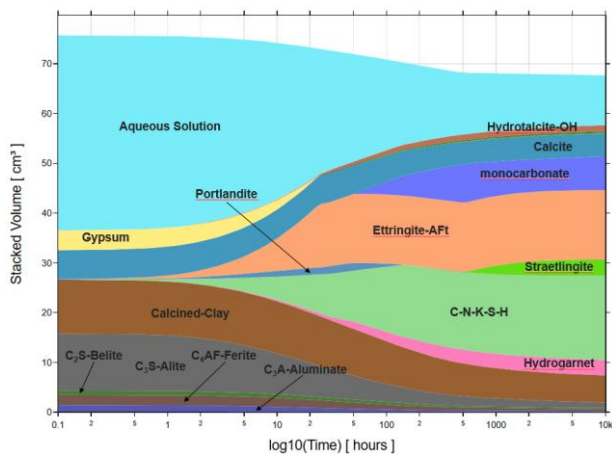


Figure 4. Thermodynamic simulation of solid phase evolution during the hydration of LC3-55.

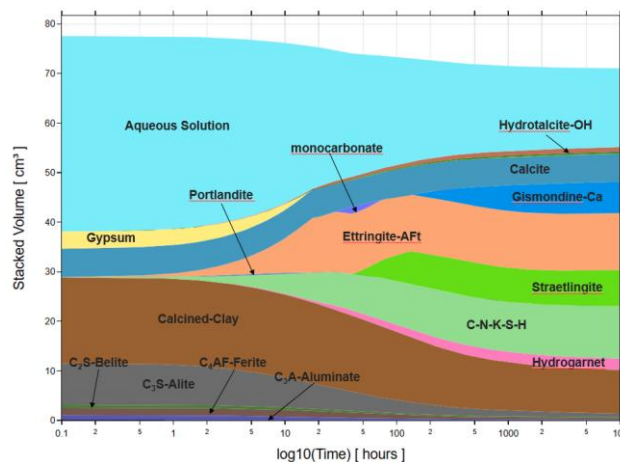


Figure 7. Thermodynamic simulation of solid phase evolution during the hydration of LC3-40.

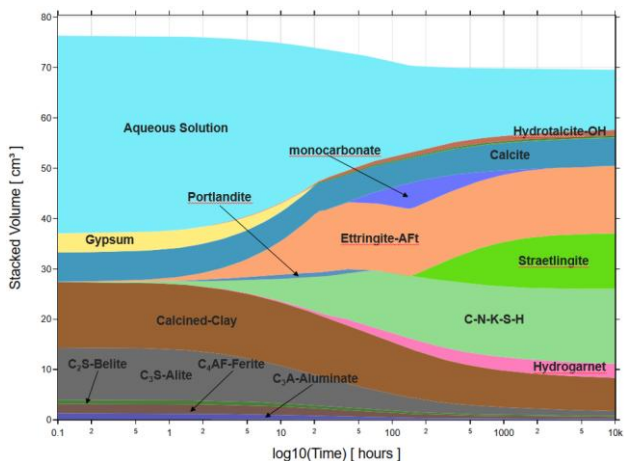


Figure 5. Thermodynamic simulation of solid phase evolution during the hydration of LC3-50.

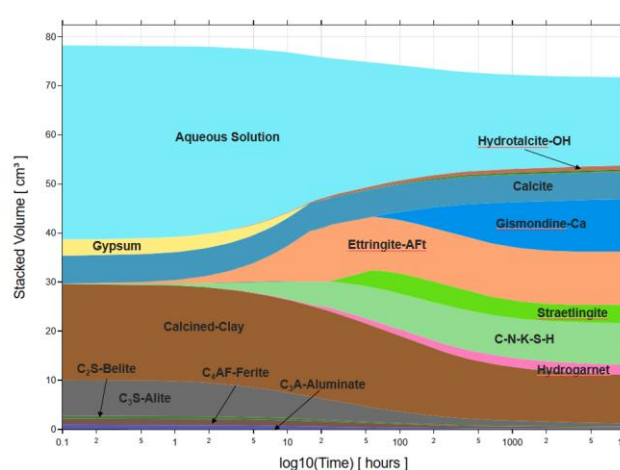


Figure 8. Thermodynamic simulation of solid phase evolution during the hydration of LC3-35.

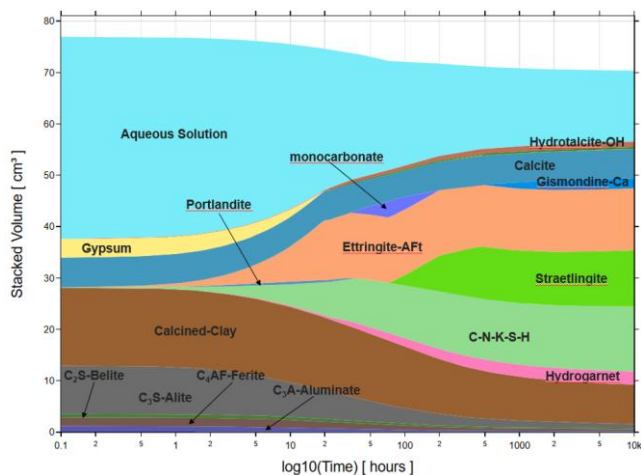


Figure 6. Thermodynamic simulation of solid phase evolution during the hydration of LC3-45.

3.1.2. Evolution of pore solution chemistry and physical properties

Table 3. Calculated pH, total volume, and solid volume of OPC and LC3 mixtures at 28 days of hydration.

System	pH	Total volume (cm ³)	Solid volume (cm ³)
OPC	13.468	66.124	56.765
LC3-65	13.432	67.828	56.621
LC3-60	13.395	68.167	56.583
LC3-55	13.315	68.444	56.320
LC3-50	13.076	68.904	55.593
LC3-45	13.075	70.624	55.320
LC3-40	12.816	71.825	54.567
LC3-35	12.818	72.629	53.247

Table 3 summarizes key calculated parameters (pH, total volume, and solid volume) at 28 days of hydration for OPC and various LC3

mixtures. As shown in Table 3, the pH values generally decrease as the clinker content is reduced from LC3-65 to LC3-35. OPC exhibits the highest pH (13.468) due to its high concentration of portlandite ($\text{Ca}(\text{OH})_2$) produced from the hydration of alite and belite. In LC3 mixtures, the inclusion of calcined clay and limestone consumes portlandite to form C-(A)-S-H and carboaluminate phases, thereby slightly decreasing the overall pH of the pore solution. LC3-50 and LC3-45 show similar pH values around 13.07, while the lowest clinker content (LC3-40 and LC3-35) results in the lowest pH, approximately 12.8. The significant reduction in pore solution pH for the low clinker mixtures, particularly reaching a minimum of 12.8 in LC3-35, warrants a careful evaluation of the matrix's alkali reserve and its implications for structural durability. In traditional OPC, a high pH (13.468) is sustained by the abundant precipitation of portlandite ($\text{Ca}(\text{OH})_2$). In the LC3 blends, the intensive pozzolanic consumption of $\text{Ca}(\text{OH})_2$ by the reactive alumina and silica from the calcined clay systematically lowers the concentration of free hydroxyl ions (OH^-) in the pore solution. From a corrosion-mitigation standpoint, although a pH of 12.8 represents a minor depletion of the alkaline buffer, it remains comfortably above the critical thermodynamic threshold (typically established at $\text{pH} \geq 11.5$) required to maintain the stability of the passive polynuclear $\text{Fe}_2\text{O}_3 \cdot \text{H}_2\text{O}$ oxide film on embedded steel reinforcement. Consequently, under non-carbonated conditions, the alkali reserve provided by the ongoing buffering capacity of the alkali-substituted C-(A)-S-H gel matrix is entirely sufficient to preserve long-term steel passivation in structural applications.

The total volume of the hydrated cement paste, solid products plus free water, shows an increasing trend with the decrease in clinker content from 67.828 cm^3 for LC3-65 to 72.629 cm^3 for LC3-35. Conversely, the calculated solid volume of hydration products at 28 days displays a downward trend as clinker loading drops, falling from 56.621 cm^3 in LC3-65 to 53.247 cm^3 in LC3-35. Nominally, this drop implies a corresponding expansion in capillary porosity, which would compromise compressive strength development. However, this physical constraint is explicitly counteracted in the intermediate formulations, establishing LC3-50 as the thermodynamic optimum. At a 50 % clinker replacement level, the system introduces an optimal stoichiometric ratio between the reactive alumina derived from the calcined clay and the carbonate ions dissolved from the limestone. This specific ratio maximizes the precipitation of the monocarboaluminate (Mc) phase, a highly hydrated crystalline compound. Because monocarboaluminate possesses a substantially high molar volume, its sustained growth acts as a highly efficient 'space-filling' mechanism within the microstructure. The morphology of the Mc phase fills the capillary voids left by the reduced C-(A)-S-H gel generation, refining the pore network and restoring solid matrix density without requiring high clinker contents.

3.2. Life cycle assessment

LCA calculation to assess the environmental impact of a cement product is a complex process and requires a comprehensive analysis

from the extraction of input materials to the final product being used and processed. From the results of the hydration process of LC3 mixtures in section 3.1.1, the optimum LC3-50 was selected for the LCA evaluation compared to that of OPC. The value of the environmental impact indicators and the emission reduction effect of LC3-50 compared to the OPC cement are shown in Figure 9 and Figure 10 respectively.

GWP is the most critical indicator for assessing climate change impact. The analysis revealed a significant difference in emissions. Particularly, $886.20 \text{ kg CO}_2 \text{ eq}$ for OPC and $594.45 \text{ kg CO}_2 \text{ eq}$ for LC3-50. This transition to the LC3 system results in an overall GWP emission reduction of up to 32.92 %. The high GWP of OPC is primarily attributed to the clinker production stage, which is energy-intensive and releases large amounts of CO_2 from the thermal decomposition of limestone and the consumption of fossil fuels required to maintain the kiln temperature (up to $1450 \text{ }^\circ\text{C}$). Conversely, LC3 exhibits lower emissions due to the reduction in clinker ratio and the use of alternative raw materials, calcined clay and limestone powder. Calcined clay requires a much lower processing temperature ($600\text{--}800 \text{ }^\circ\text{C}$), which optimizes energy efficiency during production. Because the environmental profile of calcined clay is inherently bound to the thermal energy source consumed during the $600\text{--}800 \text{ }^\circ\text{C}$ activation window, the baseline GWP reduction of 32.92 % achieved by LC3-50 remains conservative. A sensitivity consideration of the thermal inventory indicates that substituting the baseline coal-heavy mix with cleaner alternatives, such as pure natural gas or sustainably sourced biomass residues, could decrease the GWP of the clay calcination phase by an additional 15 % and 28 %, respectively. This highlights a clear optimization pathway for manufacturing plants to maximize the decarbonization potential of green cement binders via regional energy-mix transitions.

The ODP quantifies the potential damage to the stratospheric ozone layer. As shown in Figure 9, the ODP for the OPC system is $7.43\text{E-}06 \text{ kg CFC-11 eq}$, whereas the LC3-50 records an ODP of $4.40\text{E-}06 \text{ kg CFC-11 eq}$. The resulting ODP environmental reduction efficiency, illustrated in Figure 10, is 40.78 %, making it the highest reduction among the six environmental impact indicators. Maintaining the high sintering temperatures ($1450 \text{ }^\circ\text{C}$) required for traditional OPC clinker manufacturing demands extensive combustion of fossil fuels, a process fundamentally tied to elevated Ozone Depletion Potential (ODP) footprints. Within the CML 2001 baseline methodology, the ODP metric tracks trace emissions of highly stable halogenated substances, primarily Trichlorofluoromethane (CFC-11), Dichlorodifluoromethane (CFC-12), and Bromotrifluoromethane (Halon-1301), which escape into the atmosphere during both the upstream extraction/refining of heavy fuel oils and the high-temperature combustion of industrial coal within the rotary kiln. As illustrated in Figure 9, the OPC system records an ODP of $7.43\text{E-}06 \text{ kg CFC-11 eq}$. By substituting 45 % of this clinker with a combination of unheated limestone powder and clay calcined at low thermal limits ($600\text{--}800 \text{ }^\circ\text{C}$), the LC3-50 mixture significantly bypasses these intensive upstream and direct fuel combustion phases. This direct

reduction in thermal energy demand results in a remarkable 40.78 % reduction in total ODP emissions (4.40E-06 kg CFC-11 eq).

POCP reflects the potential for tropospheric pollution through ozone formation, which leads to photochemical smog, affecting human health and ecosystems. The results indicate that the LC3-50 achieves an emission reduction efficiency of 20 % compared to the OPC, as shown in Figure 10. This decline is primarily related to the reduction in fossil fuel consumption during production. The combustion of fuel at extremely high temperatures to burn clinker in the OPC system emits large amounts of NO_x gases and uncombusted compounds. These are the main precursors that undergo photochemical reactions under sunlight to form ozone. By reducing the clinker content, the LC3-50 minimizes the concentration of these precursor pollutants, thereby helping to improve the air quality around the production areas.

AP quantifies the potential to cause acid rain, which severely affects soil and aquatic ecosystems. The analysis shows that the LC3-50 has an AP value of 1.79 mol H⁺ eq, lower than the 2.39 mol H⁺ eq for the OPC cement, resulting in an AP emission reduction efficiency of 25.32 % (Figure 10). This improvement stems from the optimization of the thermal process and the reduction of the clinker ratio. High-temperature clinker production in OPC leads to large emissions of acidifying gases such as SO₂ and NO_x from the combustion of fossil fuels, which are the two main agents causing acidification. In contrast, the LC3-50 requires a lower processing temperature (600-800 °C), which limits the formation of acidifying gases and reduces the overall fuel demand. Furthermore, the use of unheated limestone powder also helps to eliminate sources of acidifying gas emissions during this stage.

EP is the phenomenon of increased nutrient levels in soil and water environments, leading to algal blooms and oxygen depletion. Based on the results presented in Figure 9, the EP values for the OPC and the LC3-50 are 8.28 mol N eq and 6.62 mol N eq, respectively. Consequently, the production of the LC3-50 achieves an EP emission reduction efficiency of 20.05 %. This improvement is primarily due to the reduced fossil fuel consumption during clinker burning. Fuel combustion at high temperatures releases nitrogen oxides (NO_x) into the atmosphere. These nitrogen oxides subsequently settle into water and soil sources as nitrogen compounds, causing eutrophication.

Fossil energy consumption is a major factor in cement production. Based on the analysis, the ADPF value for the OPC is 3504 MJ, while the LC3-50 reduces this to 2803.2 MJ. Replacing clinker with calcined clay and limestone provides a fossil resource saving efficiency of up to 20 % (Figure 10). This reflects the efficiency gained by reducing the clinker ratio and utilizing alternative raw materials in the production of environmentally friendly, green cement. It is important to note that while this study strictly enforces a standardized 'cradle-to-gate' system boundary, the long-term environmental profile of cementitious binders is influenced by their behavior during the active 'use phase.' LC3 systems generally exhibit higher carbonation rates over their service life compared to traditional OPC, a phenomenon driven by their lower residual portlandite (Ca(OH)₂) reserve which is consumed during the initial

pozzolanic reaction. Consequently, the total potential for passive CO₂ uptake via ambient carbonation during the structural service life may be reduced in LC3 systems. However, when evaluated from a full cradle-to-grave perspective, the minor deficit in use-phase carbonation uptake is completely outweighed by the massive 32.92 % upfront carbon savings achieved during clinker manufacturing. The rapid mitigation of initial emissions remains the most critical factor for satisfying immediate net-zero climate goals, confirming that the LC3-50 formulation represents an exceptional cradle-to-gate environmental asset.

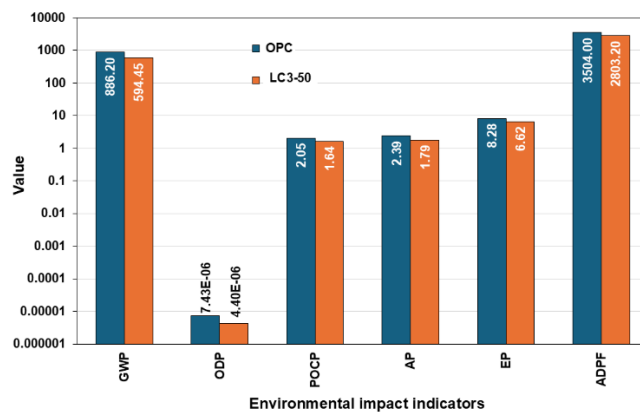


Figure 9. Comparison of environmental impact indicators between OPC and LC3-50.

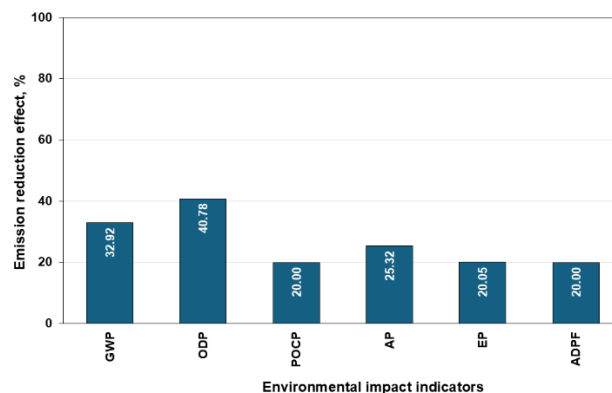


Figure 10. Percentage reduction of environmental impacts for LC3-50 compared to OPC.

4. Conclusions

This study comprehensively evaluated the microstructural evolution and environmental impact of LC3 mixtures compared to OPC by integrating thermodynamic modeling with LCA. Based on the results, the following main conclusions are drawn:

Thermodynamic simulations reveal that LC3 mixtures undergo a distinctly different hydration pathway compared to OPC. The synergistic reaction between the reactive alumina from calcined clay and the limestone effectively stabilizes the AFm phases into hemicarboaluminate and, ultimately, monocarboaluminate. This

process, coupled with the vigorous pozzolanic consumption of portlandite to form C-(A)-S-H gel, significantly refines and densifies the solid matrix.

Among the investigated range of clinker replacements, the LC3-50 mixture emerges as the thermodynamically optimal blend. It achieves a balance by maintaining sufficient C-(A)-S-H generation for structural integrity while maximizing the precipitation of space filling monocarboaluminate phases, without completely depleting the portlandite reserve necessary for systemic stability.

The LCA definitively proves the superior environmental profile of the optimized LC3-50 mixture. By reducing the clinker content and utilizing calcined clay and limestone, the LC3-50 achieves remarkable reductions across all key environmental impact indicators. Most notably, it reduces the GWP by 32.92 %, the ODP by 40.78 %, and the ADPF by 20.00 % compared to traditional OPC.

The successful coupling of thermodynamic phase predictions with environmental impact quantification demonstrates that LC3 mixtures is not merely an eco-friendly substitute but a technically robust binder. The LC3-50 formulation offers a highly viable, low-carbon pathway for the cement industry to meet the 2050 net-zero targets while ensuring long-term material performance.

References

- [1]. "Net Zero by 2050 – Analysis," IEA. Accessed: Apr. 09, 2026. [Online]. Available: <https://www.iea.org/reports/net-zero-by-2050>
- [2]. N. Dilissen, J. Vleugels, J. Vermeiren, B. García-Baños, J. R. S. Marín, and J. M. Catalá-Civera, "Temperature dependency of the dielectric properties of hydrated and ordinary Portland cement and their constituent phases at 2.45 GHz up to 1100 °C," *Cement and Concrete Research*, vol. 165, p. 107067, Mar. 2023, doi: 10.1016/j.cemconres.2022.107067.
- [3]. B. M. A. Smadi, K. K. Al-Zboon, and K. M. Shatnawi, "Assessment of Air Pollutants Emissions from a Cement Plant: A Case Study in Jordan," *Jordan Journal of Civil Engineering*, vol. 3, no. 3, Accessed: Apr. 09, 2026. [Online]. Available: <https://jjce.just.edu.jo/Home/ShowPaper.aspx?data=kNsNesCGq3XeOKpvSK7UyqSC%2BivxXzybMNIwvyLHx5w%3D>
- [4]. "Technology Roadmap - Low-Carbon Transition in the Cement Industry – Analysis," IEA. Accessed: Apr. 09, 2026. [Online]. Available: <https://www.iea.org/reports/technology-roadmap-low-carbon-transition-in-the-cement-industry>
- [5]. K. Scrivener, F. Martirena, S. Bishnoi, and S. Maity, "Calcined clay limestone cements (LC3)," *Cement and Concrete Research*, vol. 114, pp. 49–56, Dec. 2018, doi: 10.1016/j.cemconres.2017.08.017.
- [6]. G. Huang, Y. Zhuge, B. T. (Tom) Benn, and Y. Liu, "Environmental Assessment of Limestone Calcined Clay Cement in Australia," *IOP Conf. Ser.: Mater. Sci. Eng.*, vol. 1289, no. 1, p. 012082, Aug. 2023, doi: 10.1088/1757-899X/1289/1/012082.
- [7]. S. Sanchez, H. A. Machado, F. Martirena, and L. Grimmeissen, "Unlocking the Potential of LC3: Economic, Environmental, and Financial Impacts with a Novel Assessment Tool," *IOP Conf. Ser.: Earth Environ. Sci.*, vol. 1554, no. 1, p. 012113, Nov. 2025, doi: 10.1088/1755-1315/1554/1/012113.
- [8]. B. Kanagaraj, N. Anand, U. Johnson Alengaram, R. Samuvel Raj, and S. Karthick, "Limestone calcined clay cement (LC3): A sustainable solution for mitigating environmental impact in the construction sector," *Resources, Conservation & Recycling Advances*, vol. 21, p. 200197, May 2024, doi: 10.1016/j.rcradv.2023.200197.
- [9]. "Low-carbon cement for greener development in Global South," *World Economic Forum*. Accessed: Apr. 09, 2026. [Online]. Available: <https://www.weforum.org/stories/2024/06/low-carbon-cement-sustainable-development-global-south/>
- [10]. D. A. Kulik, F. Winnefeld, A. Kulik, G. D. Miron, and B. Lothenbach, "CemGEMS – an easy-to-use web application for thermodynamic modelling of cementitious materials," *RILEM Technical Letters*, vol. 6, pp. 36–52, Jun. 2021, doi: 10.21809/rilemtechlett.2021.140.
- [11]. A. Giroth, "ICT for environment in life cycle applications openLCA — A new open source software for life cycle assessment," *Int J Life Cycle Assess*, vol. 12, no. 4, pp. 209–210, Jun. 2007, doi: 10.1065/lca2007.06.337.
- [12]. "Cemdata18 database - nanocem CemGEMS." Accessed: Apr. 09, 2026. [Online]. Available: <https://cemgems.org/cemdata/about-cemdata/>
- [13]. D. A. Kulik et al., "GEM-Selektor geochemical modeling package: revised algorithm and GEMS3K numerical kernel for coupled simulation codes," *Comput Geosci*, vol. 17, no. 1, pp. 1–24, Feb. 2013, doi: 10.1007/s10596-012-9310-6.
- [14]. F. Lai et al., "Life cycle inventories of global metal and mineral supply chains: a comprehensive data review, analysis and processing," *Resources, Conservation and Recycling*, vol. 226, p. 108709, Feb. 2026, doi: 10.1016/j.resconrec.2025.108709.
- [15]. J. B. Guinee, "Handbook on life cycle assessment operational guide to the ISO standards," *Int J LCA*, vol. 7, no. 5, pp. 311–313, Sep. 2002, doi: 10.1007/BF02978897.